

STARS

University of Central Florida
STARS

Faculty Bibliography 2010s

Faculty Bibliography

1-1-2011

Multiphonon Raman scattering in graphene

Rahul Rao

Derek Tishler

University of Central Florida

Jyoti Katoch

University of Central Florida

Masa Ishigami

University of Central Florida

Find similar works at: <https://stars.library.ucf.edu/facultybib2010>

University of Central Florida Libraries <http://library.ucf.edu>

This Article is brought to you for free and open access by the Faculty Bibliography at STARS. It has been accepted for inclusion in Faculty Bibliography 2010s by an authorized administrator of STARS. For more information, please contact STARS@ucf.edu.

Recommended Citation

Rao, Rahul; Tishler, Derek; Katoch, Jyoti; and Ishigami, Masa, "Multiphonon Raman scattering in graphene" (2011). *Faculty Bibliography 2010s*. 1800.

<https://stars.library.ucf.edu/facultybib2010/1800>



Multiphonon Raman scattering in graphene

Rahul Rao,^{1,*} Derek Tishler,² Jyoti Katoch,² and Masa Ishigami²

¹*Materials and Manufacturing Directorate, Air Force Research Laboratory, Wright-Patterson AFB, OH 43433, USA*

²*Department of Physics and Nanoscience Technology Center, University of Central Florida, Orlando, FL 32816, USA*

(Received 17 June 2011; revised manuscript received 16 August 2011; published 12 September 2011)

We report on multiphonon Raman scattering in graphene samples. Higher-order combination modes involving three and four phonons are observed in single-layer, bilayer, and few-layer graphene samples prepared by mechanical exfoliation. The intensity of the higher-order phonon modes (relative to the G peak) is highest in single-layer graphene and decreases with increasing layers. In addition, all higher-order modes are observed to upshift in frequency almost linearly with increasing graphene layers, betraying the underlying interlayer van der Waals interactions.

DOI: [10.1103/PhysRevB.84.113406](https://doi.org/10.1103/PhysRevB.84.113406)

PACS number(s): 81.05.ue, 73.22.Pr, 63.22.Rc, 33.20.Fb

Single to multilayer graphene display a variety of unusual electronic and transport properties, such as Dirac physics, a tunable band gap due to the broken symmetry by additional layers, and electron interaction effects.¹ Light interaction with graphene is highly important for both graphene science and technology. Optical techniques like Raman spectroscopy reveal fundamental properties of graphene, such as doping levels and defect concentrations,² and the utility of graphene in optoelectronics seems promising. Raman spectroscopy is also the standard technique for characterizing graphene samples due to distinct features that depend strongly on the number of layers,^{3,4} as well as the stacking order in few-layer graphene (FLG).^{5–8} In particular, the second-order 2D (also called the G') peak, which occurs due to a double resonance Raman process involving intervalley scattering of an electron by two transverse optical (iTO) phonons, is the most intense feature in the Raman spectrum of single-layer graphene (SLG) on SiO₂ and can be fitted with a single Lorentzian peak.^{2,3,9} On the other hand, the 2D peak in bilayer graphene (BLG) is composed of four Lorentzian peaks and reflects the hyperbolic electronic band structure due to the stacking between two graphene layers. As the number of layers increase, the 2D peak evolves into a two-peak structure due to coupling between graphene layers in a three-dimensional (3D) crystal.^{2,10} Furthermore, the intensity of the 2D peak diminishes with respect to the G peak with increasing graphene layers and has been used to identify the number of layers in graphene samples.¹¹

While the two-phonon 2D peak has received much attention in graphene samples, higher-order modes involving multiple phonons remain unexplored. Multiphonon Raman scattering is generally weaker in bulk materials due to a vanishing density of states (DOS) for higher-order phonons.¹² Yet multiphonon Raman scattering can be observed in single-walled carbon nanotubes (SWNTs),^{13,14} multiwalled carbon nanotubes (MWNTs),¹⁵ and highly oriented pyrolytic graphite (HOPG).^{14,16} Wang *et al.*¹³ reported intense higher-order combination modes involving up to six phonons (between 2500 and 8500 cm⁻¹) in individual SWNTs, which was made possible by large resonance enhancements due to coupling with the excitation laser. On the other hand, the multiphonon modes in MWNTs¹⁵ and HOPG^{14,16} are much weaker in intensity compared to their one- or two-phonon modes and are difficult to observe. In the same vein, it is of considerable interest to determine whether such higher-order modes can also

be observed in graphene and how they evolve with increased layer stacking. Here, we show higher-order combination modes (up to four phonons) from SLG and multilayer graphene prepared by exfoliation from HOPG on SiO₂ substrates.¹⁷ We find that the multiphonon modes are most intense in SLG and decrease in intensity with increasing layers. In addition, the three-phonon modes are observed to upshift in frequency with increasing number of layers, presumably due to van der Waals interactions caused by layer stacking.

Raman spectra ($E_{\text{laser}} = 2.33$ eV) from SLG, BLG, and FLG samples are shown along with a spectrum from HOPG in Fig. 1. The first order E_{2g} mode (G peak) at ~ 1585 cm⁻¹ and the overtone of the iTO phonon mode (2D peak) at ~ 2700 cm⁻¹ exhibit frequencies and line shapes similar to those described previously^{3,5}; the 2D peaks in SLG, BLG, and FLG can be fitted with 1, 4, and 2 Lorentzian peaks, respectively. Beyond the 2D peak frequency, several weak intensity modes can be observed between 3000 and 6000 cm⁻¹. The sharp peak (single Lorentzian) of ~ 3230 cm⁻¹ is an overtone of the D' peak and is called the 2D' peak. The D' peak is a disorder-induced peak occurring ~ 1620 cm⁻¹ in sp^2 carbon samples, and is caused by double resonance *intravalley* scattering of a photoexcited electron by a phonon, along with elastic scattering by a defect. The 2D' peak at ~ 3230 cm⁻¹ is its overtone, and like the 2D peak, it does not need defects for activation. The overtone of the G peak (2G) at ~ 3160 cm⁻¹ is generally not observed in the graphite Raman spectrum,¹⁸ although it has been observed previously in the resonance Raman spectra from SWNTs.¹³ Hence, as described later, we assign some higher-order modes above 4500 cm⁻¹ to combinations involving the 2D' peak rather than to those involving the 2G peak, as assigned by earlier reports.^{15,16}

Beyond 4000 cm⁻¹, a peak at ~ 4250 cm⁻¹ is the most intense feature in the Raman spectra shown in Fig. 1. This feature is assigned to a combination of the G and 2D modes (G + 2D), as explained further later.¹⁹ The intensity of the G + 2D peak is highest for SLG and decreases in intensity with increasing layers, tracking the intensity of the 2D peak, which is also the most intense for SLG compared to multilayer graphene. A weak intensity peak at ~ 4030 cm⁻¹ is also observed in all samples and is assigned to a combination of the D and 2D modes (D + 2D). Both the G + 2D and the D + 2D peaks are shown more clearly in Fig. 2, where the spectra have been normalized by the intensity of the G + 2D peak and fitted

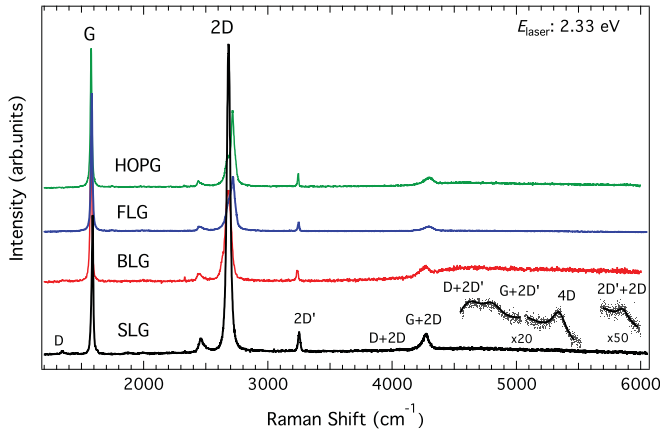


FIG. 1. (Color online) Higher-order Raman spectra from graphene samples collected with $E_{\text{laser}} = 2.33$ eV. All spectra have been normalized by the G peak intensity. Some weak intensity combination modes appearing above 4500 cm^{-1} are magnified for clarity.

with Lorentzian peaks. The G + 2D peak in SLG can be fit with a single Lorentzian peak; hence, its line shape is similar to that of the 2D peak in SLG. However, the line width of the G + 2D peak (full width at half maximum, or FWHM $\approx 85\text{ cm}^{-1}$) is greater than the 2D peak (FWHM $\approx 30\text{ cm}^{-1}$). On the other hand, the G + 2D peaks in BLG, FLG, and HOPG can be deconvoluted into multiple peaks, reflecting the changes in the electronic band structure brought about by coupling between graphene layers; this is also observed in the 2D peak from BLG and FLG samples.^{2,3,9} The assignments of the G + 2D and D + 2D peaks can be confirmed by the dispersion of the peaks with increasing laser energy ($E_{\text{laser}} = 2.33, 2.54,$

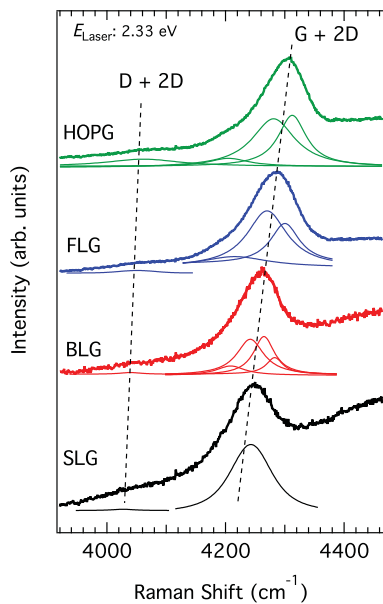


FIG. 2. (Color online) Higher-order combination modes between 4000 and 4400 cm^{-1} in graphene samples collected with $E_{\text{laser}} = 2.33$ eV. All spectra have been normalized with respect to the G + 2D peak intensity for clarity and have been fitted with Lorentzian peaks. The D + 2D and G + 2D peaks upshift in frequency with increasing layers.

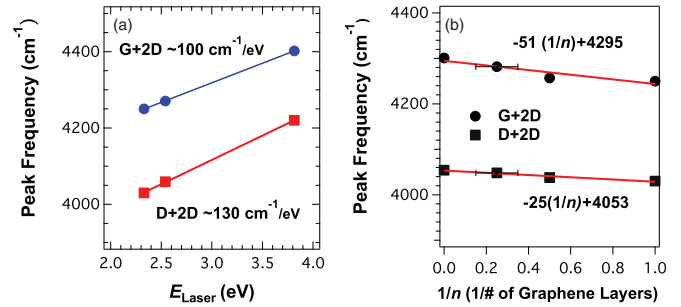


FIG. 3. (Color online) (a) Dispersion of the G + 2D and D + 2D peaks in SLG versus laser energy. (b) Peak frequencies of the G + 2D and D + 2D peaks versus $1/n$. The error bars for the FLG samples were obtained from atomic force microscopy (AFM) measurements, which confirmed the presence of three to five layers.

and 3.81 eV), as shown in Fig. 3(a). The dispersion of the G + 2D peak is $\sim 100\text{ cm}^{-1}/\text{eV}$, which should be similar to the dispersion of the 2D peak ($\sim 95\text{ cm}^{-1}/\text{eV}$), because the G peak is dispersionless. On the other hand, the dispersion of the D + 2D peak should approximately equal the sum of the dispersions of the D (typically $\sim 50\text{ cm}^{-1}/\text{eV}$)²⁰ and 2D ($\sim 95\text{ cm}^{-1}/\text{eV}$) peaks and is found to be $\sim 130\text{ cm}^{-1}/\text{eV}$. Similar dispersions can be observed for the G + 2D peak in BLG, as shown in Fig. 4. The G + 2D peak in BLG can be deconvoluted into four peaks, similar to the 2D peak in BLG.^{3,9} The dispersions of the four components within the 2D peak have been reported to vary between 80 and $100\text{ cm}^{-1}/\text{eV}$.²¹⁻²³ As shown in Fig. 4, the dispersion of the highest frequency component within the G + 2D peak in BLG is $\sim 98\text{ cm}^{-1}/\text{eV}$, and the dispersions of the other peaks within the G + 2D and 2D peaks are similar. Moreover, the differences in frequencies among the four components of the G + 2D peak ($\sim 20\text{--}40\text{ cm}^{-1}$) are similar to those among the four components in the 2D peak in BLG.

Another interesting feature that can be observed in the spectra shown in Fig. 2 (indicated by the dotted lines) is that the G + 2D and D + 2D peaks appear to upshift in frequency

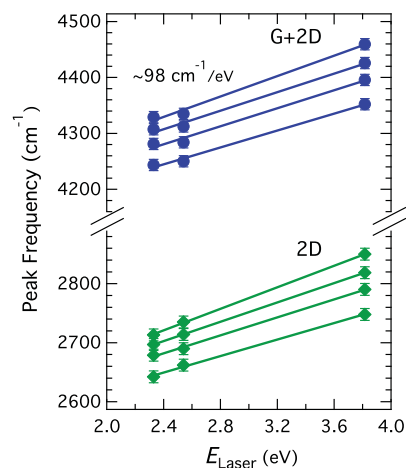


FIG. 4. (Color online) Dispersion of four components within the G + 2D and 2D peaks in BLG versus laser energy. The dispersion of the highest frequency component in the G + 2D peak ($\sim 98\text{ cm}^{-1}/\text{eV}$) is indicated in the figure.

with increasing graphene layers. Such upshifts with increasing graphene layers have been observed recently for combination modes between 1700 and 2300 cm^{-1} involving optical and acoustic phonons,⁵ as well as for the G peak phonons in exfoliated graphene.⁴ As shown in the plot of peak frequencies versus number of layers ($1/n$) in Fig. 3(b), the G + 2D and D + 2D peaks exhibit an almost linear dependence on $1/n$ and the data can be fitted by an equation of the form $\omega(n) = \beta/n + \omega(\infty)$, where n is the number of graphene layers and β is a constant.⁴ The values of β (50 and 25 cm^{-1} for the G + 2D and D + 2D peaks, respectively) obtained from the linear fits in Fig. 3(b) are comparable to those reported for combination modes in graphene.⁵ Frequency upshifts of the G band in SLG ($\leq 13 \text{ cm}^{-1}$) have been found to occur due to unintentional doping.²⁴ However, in addition to an upshift in the G peak frequency, there is a corresponding narrowing of the G peak and decrease in the 2D peak intensity with unintentional (and inhomogeneous) doping.²⁴ In all the spectra used in this study, we confirmed the consistency of the G peak line width (e.g., FWHM $\approx 9\text{--}11 \text{ cm}^{-1}$ in SLG), as well as the ratio of intensities between the 2D and the G peaks among all samples and multiple spots measured on each sample. The frequency upshifts shown in Fig 3(b) are likely due to van der Waals interactions in layered systems and have been observed recently in the phonon modes of few-layer MoS₂ samples.²⁵

Finally, we turn our attention to several weak intensity modes observed above 4500 cm^{-1} in the Raman spectrum of SLG (Fig. 1). The first two peaks occur ~ 4600 and $\sim 4800 \text{ cm}^{-1}$ (see magnified peaks in Fig. 1) and are assigned to combinations of the D and 2D' (D + 2D') and G and 2D' peaks (G + 2D'), respectively. These peaks were previously assigned to the D + 2G^{15,16} and 3G¹³ peaks, respectively. Tan *et al.* observed a peak at 4800 cm^{-1} in SWNTs (with 488-nm laser excitation) and assigned it to the G + 2D' peak.¹⁴ As mentioned previously and as seen in the spectra in Fig. 1, we do not observe the overtone of the G peak (2G), which occurs at $\sim 3160 \text{ cm}^{-1}$. In addition, the expected sum of peak frequencies for the D ($\sim 1345 \text{ cm}^{-1}$) and 2D' ($\sim 3232 \text{ cm}^{-1}$) peaks is $\sim 4577 \text{ cm}^{-1}$, which is $\sim 50 \text{ cm}^{-1}$ higher than the sum of frequencies of the D and 2G peaks. Our observed peak frequency in SLG is $\sim 4600 \text{ cm}^{-1}$, which is closer to the sum

of frequencies for the D and 2D' peaks. For the preceding reasons, we assign the two peaks at ~ 4600 and $\sim 4800 \text{ cm}^{-1}$ to the D + 2D' and G + 2D' peaks, respectively. The next weak intensity mode in SLG appears at $\sim 5330 \text{ cm}^{-1}$ and is the fourth harmonic of the D peak. The occurrence of a three-phonon (3D) peak is improbable due to the requirement of momentum conservation in the scattering process.¹³ Thus, the next observable overtone of the D peak phonon is the four-phonon overtone of the D peak (four iTO phonons with equal and opposite momentum) at $\sim 5330 \text{ cm}^{-1}$ and is called the 4D peak.^{14,16,26}

The final four-phonon peak appears at $\sim 5850 \text{ cm}^{-1}$ and was previously assigned to a combination of 2G and 2D phonons in graphite and SWNTs.^{14,16} This peak is very weak in intensity and is shown magnified 50 \times in Fig. 1. To be consistent with our earlier reasoning concerning the 2G and 2D' peaks, and because the intensity of the peak at 5300 cm^{-1} is very weak, we assign the four-phonon peak at $\sim 5850 \text{ cm}^{-1}$ to the 2D' + 2D mode. Due to increasing background scattering from the SiO₂ substrate, higher-order combination modes beyond 6000 cm^{-1} involving five or six phonons are difficult to observe in our samples. Furthermore, the weak intensity three- and four-phonon modes above 4500 cm^{-1} are only observed from SLG and are difficult to resolve in multilayer graphene samples. This is due to larger resonance enhancement for phonon modes in SLG. For example, the high intensity 2D peak in SLG has been attributed to occur due to a triple resonance process, where all steps in the typical double resonance process are resonant.² Thus, we would expect the intensities of higher-order combination modes involving the 2D phonon to also be higher than the corresponding peaks in BLG, FLG, and HOPG samples. This might explain why the higher-order combination modes are observed in SLG but are very weak in intensity in multilayer graphene. All the multiphonon peaks described previously are listed in Table I, along with peak assignments and expected frequencies (based on the sum of the individual components). Also included in Table I are experimentally observed multiphonon peaks in HOPG for comparison.

In summary, we report multiphonon Raman modes (three- and four-phonon modes) in SLG, BLG, and FLG samples

TABLE I. Peak frequencies and assignments for the multiphonon modes observed in SLG ($E_{\text{laser}} = 2.33 \text{ eV}$) and experimentally observed multiphonon peaks in HOPG ($E_{\text{laser}} = 2.41 \text{ eV}$) taken from Ref. 9.

Peak frequency (cm^{-1})	Peak assignment	Expected) frequency (cm^{-1})	Corresponding peaks observed in HOPG ⁹
1345	D	1345	1352
1583	G	1580	1580
1620	D'	1620	1622
2675	2D	2690	2705
3232	2D'	3240	3244
4030	D + 2D	4035	4031
4250	G + 2D	4270	4288
4600	D + 2D'	4585	4544
4800	G + 2D'	4820	4830
5330	4D	5380	5370
5857	2D' + 2D	5930	5870

on SiO₂ substrates. Peak assignments are made based on the dispersion of the peaks versus laser excitation energy, as well as the expected frequency obtained from the sum of the individual components. The D + 2D and G + 2D peak frequencies are observed to have an almost-linear dependence on the number of graphene layers, suggesting an influence of interlayer van der Waals interactions on the peak frequencies. The distinct layer dependence of the G + 2D peak frequency provides another metric for the correct identification of the number of layers in graphene samples. Higher-order four-phonon modes are also observed in SLG, although these peaks are much weaker in intensity in graphene samples with two or more layers due to the large resonance enhancement in SLG. The peak frequencies of all combination modes in SLG are also shifted relative to the same modes observed previously in

SWNTs; e.g., the G + 2D peak in SWNTs has been observed at $\sim 4300\text{ cm}^{-1}$ (with $E_{\text{laser}} = 2.41\text{ eV}$),^{13,14} while the same peak in SLG occurs at $\sim 4260\text{ cm}^{-1}$ with the same laser excitation. This confirms the uniqueness of the phonon band structure of this one-atom-thick, two-dimensional material, which is different from both one-dimensional SWNTs and 3D graphite.

ACKNOWLEDGMENTS

R.R. is grateful for funding from the Air Force Office of Scientific Research and the National Research Council associateship program and thanks Humberto Gutierrez for assistance with part of the Raman spectroscopy measurements. D.T., J.K., and M.I. are supported by the National Science Foundation under Grant No. 0955625.

*rrao@honda-ri.com, present address: Honda Research Institute, 1381 Kinnear Rd., Columbus, OH.

¹A. K. Geim and K. S. Novoselov, *Nat. Mater.* **6**, 183 (2007).

²L. Malard, M. Pimenta, G. Dresselhaus, and M. Dresselhaus, *Phys. Rep.* **473**, 51 (2009).

³A. C. Ferrari, J. C. Meyer, V. Scardaci, C. Casiraghi, M. Lazzeri, F. Mauri, S. Piscanec, D. Jiang, K. S. Novoselov, S. Roth, and A. K. Geim, *Phys. Rev. Lett.* **97**, 187401 (2006).

⁴A. Gupta, G. Chen, P. Joshi, S. Tadigadapa, and P. Eklund, *Nano Lett.* **6**, 2667 (2006).

⁵R. Rao, R. Podila, R. Tsuchikawa, J. Katoch, D. Tishler, A. M. Rao, and M. Ishigami, *ACS Nano* **5**, 1594 (2011).

⁶C. Cong, T. Yu, R. Saito, G. F. Dresselhaus, and M. S. Dresselhaus, *ACS Nano* **5**, 1600 (2011).

⁷P. Poncharal, A. Ayari, T. Michel, and J. L. Sauvajol, *Phys. Rev. B* **78**, 113407 (2008).

⁸P. Poncharal, A. Ayari, T. Michel, and J. L. Sauvajol, *Phys. Rev. B* **79**, 195417 (2009).

⁹J. Park, A. Reina, R. Saito, J. Kong, G. Dresselhaus, and M. Dresselhaus, *Carbon* **47**, 1303 (2009).

¹⁰E. Barros, N. Demir, A. Souza Filho, J. Mendes Filho, A. Jorio, G. Dresselhaus, and M. Dresselhaus, *Phys. Rev. B* **71**, 165422 (2005).

¹¹I. Calizo, I. Bejenari, M. Rahman, G. Liu, and A. A. Balandin, *J. Appl. Phys.* **106**, 043509 (2009).

¹²B. A. Weinstein and M. Cardona, *Phys. Rev. B* **7**, 2545 (1973).

¹³F. Wang, W. Liu, Y. Wu, M. Y. Sfeir, L. Huang, J. Hone, S. O'Brien, L. E. Brus, T. F. Heinz, and Y. R. Shen, *Phys. Rev. Lett.* **98**, 047402 (2007).

¹⁴P. Tan, Y. Tang, Y. M. Deng, F. Li, Y. L. Wei, and H. M. Cheng, *Appl. Phys. Lett.* **75**, 1524 (1999).

¹⁵W. Li, H. Zhang, C. Wang, Y. Zhang, L. Xu, K. Zhu, and S. Xie, *Appl. Phys. Lett.* **70** (1997).

¹⁶Y. Kawashima and G. Katagiri, *Phys. Rev. B* **52**, 10053 (1995).

¹⁷The graphene samples were prepared by mechanical exfoliation of HOPG on silicon/silicon dioxide substrates. Atomic force microscopy was used to confirm the presence of a single layer, bilayer, and few layers (see Supplementary Information in Ref. 3). The FLG samples typically consisted of three to five layers. Micro-Raman characterization using 325-, 488-, and 532-nm laser excitation was performed with a Renishaw inVia Raman microscope.

¹⁸C. Thomsen, *Phys. Rev. B* **61**, 4542 (2000).

¹⁹J. Charlier, P. C. Eklund, J. Zhu, and A. C. Ferrari, in *Carbon Nanotubes: Advanced Topics in the Synthesis, Structure, Properties and Applications*, edited by A. Jorio, G. Dresselhaus, and M. S. Dresselhaus (Springer-Verlag, Berlin, 2008), p. 673.

²⁰A. K. Gupta, Y. Tang, V. H. Crespi, and P. C. Eklund, *Phys. Rev. B* **82**, 241406 (2010).

²¹L. M. Malard, J. Nilsson, D. C. Elias, J. C. Brant, F. Plentz, E. S. Alves, A. H. Castro Neto, and M. A. Pimenta, *Phys. Rev. B* **76**, 201401 (2007).

²²L. Cançado, A. Reina, J. Kong, and M. Dresselhaus, *Phys. Rev. B* **77**, 245408 (2008).

²³D. L. Mafra, E. A. Moujaes, S. K. Doorn, H. Htoon, R. W. Nunes, and M. A. Pimenta, *Carbon* **49**, 1511 (2011).

²⁴C. Casiraghi, S. Pisana, K. Novoselov, A. Geim, and A. Ferrari, *Appl. Phys. Lett.* **91**, 233108 (2007).

²⁵C. Lee, H. Yan, L. E. Brus, T. F. Heinz, J. Hone, and S. Ryu, *ACS Nano* **4**, 2695 (2010).

²⁶P. Tan, S. Dimovski, and Y. Gogotsi, *Philos. Trans. R. Soc. London A* **362**, 2289 (2004).